

2024-02-06

# The assessment of neuronal plasticity following sciatic nerve injuries in rats using electron microscopy and stereological methods

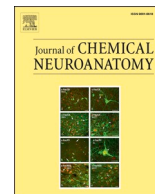
Delibas, Burcu

Elsevier

---

<https://doi.org/10.1016/j.jchemneu.2024.102396>

*Provided with love from The Nelson Mandela African Institution of Science and Technology*



## Review Article

# The assessment of neuronal plasticity following sciatic nerve injuries in rats using electron microscopy and stereological methods

Burcu Delibaş<sup>a</sup>, John-Mary Vianney<sup>b</sup>, Süleyman Kaplan<sup>b,c,\*</sup>

<sup>a</sup> Department of Histology and Embryology, Faculty of Medicine, Recep Tayyip Erdoğan University, Rize, Türkiye

<sup>b</sup> School of Life Science and Bioengineering, Nelson Mandela-African Institution of Science and Technology, Arusha, Tanzania

<sup>c</sup> Department of Histology and Embryology, Faculty of Medicine, Ondokuz Mayıs University, Samsun, Türkiye



## ARTICLE INFO

## Keywords:

Dorsal root ganglia  
Histomorphometry  
Nerve fibers  
Nerve regeneration  
Stereology

## ABSTRACT

The transmission of signals to the cell body from injured axons induces significant alterations in primary sensory neurons located in the ganglion tissue, the site of the perikaryon of the affected nerve fibers. Disruption of the continuity between the proximal and distal ends leads to substantial adaptability in ganglion cells and induces macrophage-like activity in the satellite cells. Research findings have demonstrated the plasticity of satellite cells following injury. Satellite cells work together with sensory neurons to extend the interconnected surface area in order to permit effective communication. The dynamic cellular environment within the ganglion undergoes several alterations that ultimately lead to differentiation, transformation, or cell death. In addition to necrotic and apoptotic cell morphology, phenomena such as histomorphometric alterations, including the development of autophagic vacuoles, chromatolysis, cytosolic degeneration, and other changes, are frequently observed in cells following injury. The use of electron microscopic and stereological techniques for assessing ganglia and nerve fibers is considered a gold standard in terms of investigating neuropathic pain models, regenerative therapies, some treatment methods, and quantifying the outcomes of pharmacological and bioengineering interventions. Stereological techniques provide observer-independent and reliable results, which are particularly useful in the quantitative assessment of three-dimensional structures from two-dimensional images. Employing the fractionator and disector techniques within stereological methodologies yields unbiased data when assessing parameters such as number. The fundamental concept underlying these methodologies involves ensuring that each part of the structure under evaluation has an equal opportunity of being sampled. This review describes the stereological and histomorphometric evaluation of dorsal root ganglion neurons and satellite cells following nerve injury models.

## 1. Introduction

### 1.1. Sciatic nerve injury types

The sciatic nerve, one of the largest nerves in the body, is susceptible to various types of injuries (e.g., tumor excision lesions, work accidents, compression, laceration, etc.). The severity of injury can be mild, moderate or severe according to the injury type and affected body parts. Two classification systems are still acceptable regarding injury type classifications. Seddon classified nerve injuries as neuropraxia (*Aegypt. Neur, nerve/ apraxis, inaction*), axonotmesis (*Aegypt. Axono, axon/ thmesis, incision*) and neurotmesis (*Aegypt. Neuro, nerve/ thmesis, incision*), whereas Sunderland increased Seddon's classification to five

according to the type of trauma and severity of injury to the tissues. The first-degree injury type in Sunderland's classification is equivalent to Seddon's neuropraxia type injury, resulting in only temporary conduction disturbance due to demyelination and recovery is usually complete. Sunderland's second-degree injury type is equivalent to Seddon's axonotmesis-type injuries. In such injuries, axonal integrity is impaired, but the endoneurium is intact. Axonal regeneration is easy due to the integrity of the endoneurium. In Sunderland's 3rd degree injury type, the axon and myelin sheath, including the endoneurium, are damaged, but the perineurium remains intact and full recovery is not observed in this type of injury. In Sunderland's 4th degree injury type, the myelin sheath, axon, endoneurium, and perineurium are damaged. Nerve continuity is provided only by the epineurium and spontaneous recovery is

\* Corresponding author at: Department of Histology and Embryology, Faculty of Medicine, Ondokuz Mayıs University, Samsun, Türkiye.  
E-mail addresses: [skaplan@omu.edu.tr](mailto:skaplan@omu.edu.tr), [skaplanomu@yahoo.com](mailto:skaplanomu@yahoo.com) (S. Kaplan).

<https://doi.org/10.1016/j.jchemneu.2024.102396>

Received 18 December 2023; Received in revised form 1 February 2024; Accepted 4 February 2024

Available online 6 February 2024

0891-0618/© 2024 Elsevier B.V. All rights reserved.

not possible. Sunderland's grade 5 type of injury is equivalent to Seddon's neurotmesis type classification, meaning that the nerve is completely severed and complete functional loss occurs. Spontaneous recovery is not possible, and surgery is required (Seddon, 1942; Sunderland, 1951).

Investigation of the injury types using *in vivo* models is critical for the clinical translation of these injury types. Compression lesions are one of the widely used injury types that can be obtained by crushing the epineurium via various surgical tools (Delibas et al., 2021; Serger et al., 2022; Su et al., 2019). These crush injury models can be used to mimic axonotmesis-type injuries where the axonal integrity is disrupted, but the connective tissue surrounding the nerve tract remains intact. On the other hand, most severe injuries in the nerve can be seen in complete transection injuries, where the axonal integrity and the connective tissue integrity are disrupted. In this injury model, the continuity between distal and proximal stumps is totally impaired. The reunion is prevented via suturing the proximal or distal stump to a neighboring muscle (Delibas and Kaplan, 2023; Geuna, 2015). Besides these injury models, there are various injury models that mimic chronic compression injury (Li et al., 2015; Delibas and Kaplan, 2023) and end-to-end neurotmesis (Felix et al., 2013). There are various *in vivo* experimental model types for nerve regeneration studies. The evaluation of the regeneration can be performed using different assessment techniques (functional, behavioral, histological, morphological, electrophysiological, DNA, and protein-based analysis, etc.). Although the physiological, functional, and cellular outcomes can be obtained using several techniques, evaluation of the morphological data using quantitative approaches is the gold standard.

### 1.2. The dorsal root ganglion tissue following the injury

Dorsal root ganglion tissue has been widely used in studies of regeneration/degeneration. Morphological alterations following axonal injury have attracted particular attention. Neuroplasticity, a term denoting neurons' capacity to adapt and change in response to novel conditions, encompasses a broad spectrum of mechanisms. These mechanisms include not only morphological changes but also biochemical and pharmacological adaptations. Furthermore, neuroplasticity involves modifications in neuronal networks, including changes in connectivity, dendritic remodeling, and the number and morphology of dendritic spines.

Additionally, it encompasses the generation of new neurons, a process known as adult neurogenesis. Importantly, neuroplasticity is closely linked to functional recovery, as it can induce adaptive behavioral changes and predispose functional systems to adaptive plasticity. Consequently, the adaptation of the neuron to new physiological conditions leads to various numerical and morphological changes to occurring in satellite cells and neurons associated with axons following axonal injury. A dramatic increase takes place in the number of macrophages and satellite cells (Pannese, 1981; Yu et al., 2020; Zhang et al., 1997). The proliferation of macrophages may derive from the mitotic division of the resident macrophages, from the peripheral circulation (Feng et al., 2023; Guimaraes et al., 2023; Iwai et al., 2021; Yu et al., 2020). Studies showed that satellite cells express common progenitor markers with satellite glial cells, and following the injury, satellite glial cells express macrophage genes. This would be evidence for the transformation of these two cells into each other (Feng et al., 2023). Transformations and proliferation of these cells are induced by various inflammatory agents or neurotrophic factors (Chadwick et al., 2008; Hall and Landis, 1992; Lawrence, 2009; Li et al., 2015; Wee Yong, 2010). Interleukin-1 beta, TNF-alpha, transforming growth factors, s-100 proteins, and several cell adhesion molecules are regarded as the most important of these (Levy Bde et al., 2007; Sandelin et al., 2004; Xian and Zhou, 1999; Grothe et al., 1997; Takeda et al., 2007; Zhang et al., 2000; Gehrmann et al., 1991).

The up/down regulation of these molecules and various enzymes

(nucleases and proteases) leads to several morphological changes in the sensory neurons and satellite cells. The chromatolysis response, primarily characterized as the reorganization of Nissl bodies and the relocation of the structures responsible for protein synthesis within the cell, is one of the most remarkable morphological changes (Lieberman, 1971). Fragmentation in the granular endoplasmic reticulum and disruption in polyribosomal structures have been previously demonstrated as a result of this process at electron microscopic analyses (Dentinger et al., 1979). The morphological changes observed in the cell vary depending on the type of damage, with mild axonal injuries (segmental demyelination, e.g., neuropraxia) being reversible but becoming permanent when the damage is more severe (anatomical disruption of the nerve trunk, e.g., neurotmesis, severe compression, transection, laceration et cetera) (Cragg, 1970; Engh and Schofield, 1972). Another morphological change observed following injury is the presence of large vacuoles, the size of which increases in proportion to the severity of the damage. These vacuole structures are apparent not only in sensory neurons, but also in satellite cells. Satellite cells in the sensory ganglia wrap around sensory neurons, usually in a single lamellar sheath form. In the case of injury, the number of lamellar sheaths increases and displays different folding patterns and structural changes (Delibas and Kaplan, 2023).

Previous studies demonstrated that a variety of toxicologic and neuropathologic conditions lead to vacuolization of sensory neurons (Beiswanger et al., 1993; Cavaletti et al., 2007; Melli et al., 2008). Besides, some chemotherapeutic agents and exposure to toxic agents (e.g., 3-acetylpyridine) have been reported to develop small vacuoles due to decreased Na/K-ATPase activity (Beiswanger et al., 1993). Despite the distinct ultrastructural morphological features of the intracytoplasmic neuronal vacuoles, there is currently no substantiated evidence regarding their origin (Butt, 2010).

The morphological changes described above can be evaluated using qualitative histopathological techniques. Assessment tools in peripheral nerve studies can include the neuron number, neuron size, myelinated/unmyelinated axon number, the diameter of the nerve fibers, or the myelin sheath thickness. In order to estimate these parameters in an unbiased manner, researchers need to adopt quantitative approaches. Design-based stereology provides accurate quantitative structural information from tissue sections. By integrating statistical sampling methodology with geometric analysis of tissue microstructure, these tools possess the sensitivity needed to detect even minor changes. Unlike other morphometric methods that rely on tissue section analysis, design-based stereology provides statistically valid estimates that are truly three-dimensional and representative of the entire organ. Moreover, the predictability of the precision in the stereological analysis process enables the design and empowerment of studies aimed at detecting subtle variations. Stereological techniques allow researchers to estimate 3D parameters using 2D histomorphometric properties. Design-based stereological techniques can be applied to peripheral nerve tissues and ganglia for the precise estimation of parameters such as number, size, and volume (Brown et al., 2020; Canan et al., 2008). Morphological alterations in nerve and ganglion tissues can also be quantitatively assessed and measured using stereological methods. Expressing these structural changes as quantitative data can be used to determine the success of therapeutic methods or to evaluate the severity of the injury. This article discusses using stereological methods to quantitatively assess morphological changes in ganglion tissue following axonal injury.

### 1.3. The ratio of satellite cells to neurons

Under normal physiological conditions, satellite cells envelop sensory neurons in a single, thin layer. Following axonal injury, the number of satellite cells and the pattern with which they surround the neuron both change (Terry et al., 1987; Delibas and Kaplan, 2023). In addition to injury, the quantitative ratio between sensory neurons and satellite cells also changes during ganglion development. In the early stages of

development, satellite cells are fewer in number compared to neurons. However, in the later stages of development, their numbers can increase through the transformation of undifferentiated cells in the environment into satellite cells or through the mitotic division of existing satellite cells (Carr and Simpson, 1978). Several studies have provided evidence that the number of satellite cells associated with dorsal root ganglion neurons is directly correlated with the volume and surface area of those neurons (Humbertson et al., 1969; Pannese, 1960). The interrelationships among the surface area, the volume of the satellite cell sheath, and the associated neuronal body may provide insights into the mechanisms that regulate the growth of neuroglia and nervous tissues during ganglionic development, as well as shedding light on the functional significance of satellite cells in the sensory ganglia.

Light microscopy is not suitable for this purpose due to the significant variation in the thickness of satellite cell sheaths across different regions, which is below the resolving power of such devices. Additionally, the boundary between the satellite cell sheath and neuronal perikaryon frequently exhibits a complex course, primarily due to the presence of perikaryal projections, only a subset of which can be discerned using light microscopy. The relationships between the volume of the satellite cell sheath and the associated perikaryon can therefore only be accurately determined by means of electron microscopy. The ratio of satellite cells to neurons can be calculated using the test point counting grid of the Cavalieri method (Fig. 1). The Cavalieri principle is a method for calculating the volume of a structure sectioned into parallel sections at equal intervals. In order to calculate the volume of a structure using this method, the sum of the total sectioned surface area of the region in the parallel sections should be calculated. This total sectioned surface area is multiplied by the average section thickness to yield the volume of the structure in question. A point counting grid can be used for area

estimations. These grids consist of equally spaced “+” signs. Each area between these signs represents a unit square with a fixed interval (d). This unit square or quadrilateral is known as the ‘area associated per point’ [a(p)].

The number of points hitting the image depends on the size of the cross-section and the distance between the points. The area (A) of the cross-sectional image can be calculated by multiplying the total number of points counted ( $\Sigma P$ ) and the area represented by a point [a(p)] (Sonmez et al., 2010). This is formulated as

$$A = \sum P \cdot [a(p)]$$

#### 1.4. Use of the vertical rotator technique in calculating sensory neuron volumes

The vertical rotator technique is a convenient tool for estimating the perikaryon volume of ganglion cells (Jensen and Gundersen, 1993). Measurements can be performed on vertical sections sampled by optical dissectors (Baddeley et al., 1986). The nucleator and rotator principles are stereological methods used for estimating the mean volume of particles. In order to apply either principle, a unique reference point must be associated with each particle. This reference point is typically the nucleolus of the cell. All sections must be obtained parallel to the vertical axis (but can be selected arbitrarily), and all subsequent measurements must be performed relative to the axis. Using vertical “bars” is the most efficient and simplest way of applying this approach (Fig. 2).

#### 1.5. The estimation of the mitochondrial volume ratio

Mitochondrial disorders are a diverse group of diseases that can affect multiple organ systems and present with a wide range of clinical symptoms (Gorman et al., 2016; Wallace, 1999). Ultrastructural analysis has shown that mitochondrial morphology is frequently abnormal in

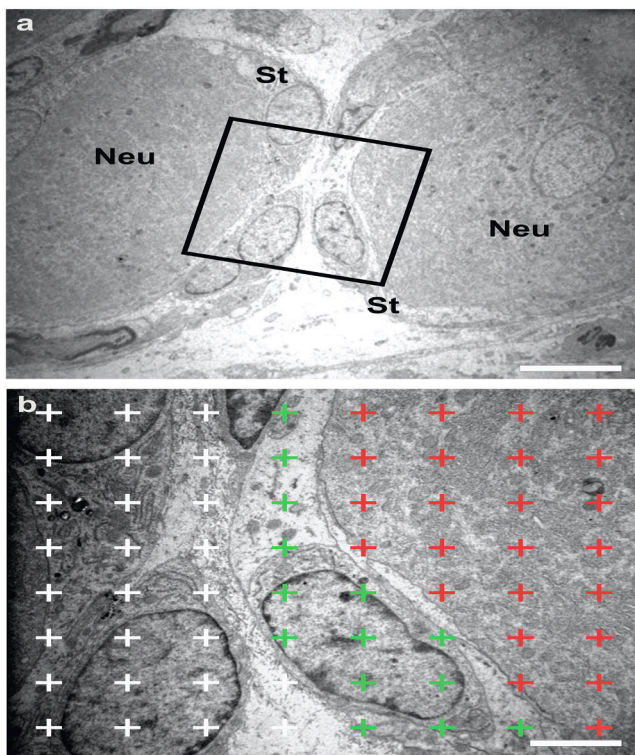


**Fig. 1.** : The figure shows the application of Cavalieri's principle for estimating the ratio of satellite cells to neurons. (a) This image shows two neurons (Neu) and the satellite cells (St) surrounding them (bar: 10  $\mu$ m). The boxed area can be seen at high magnification in the lower photograph. (b) The red (+) signs represent the intersection of the neuron with the counting grid, while the green (+) signs represent the intersection of the satellite cell with the counting grid (scale: 2  $\mu$ m).

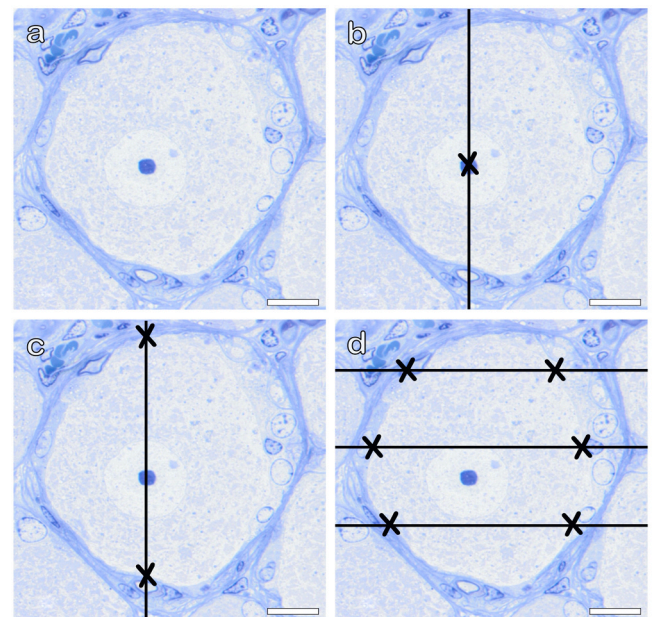


**Fig. 2.** : Application of the vertical rotator technique in estimating neuronal size. (a, b) A line parallel to the vertical axis was drawn using the nucleolus as the reference point. (c) The upper and lower ends of the perikaryon of the ganglion cell were drawn using the mouse and recorded with the software. The line was divided into two half-planes by the system. (d) Parallel and uniform test lines were applied to the neuron, and the intersection with the neuronal border and test lines was determined by the researcher. All intersections (crosses) between the profile boundary and the horizontal line are displayed (bar: 10  $\mu$ m).



these disorders, with mitochondria appearing swollen and possessing unusual and sparse cristae (Delibaş and Kaplan, 2023). This highlights the importance of morphological analysis in the diagnosis of mitochondrial disorders (Brantova et al., 2006). Additionally, the shape and size of mitochondria can vary depending on the tissue type and in response to physiological, pathological, and metabolic changes. For example, mitochondrial permeability transition (MPT) is a process in which the inner mitochondrial membrane loses its selective permeability, resulting in swelling of the mitochondrial matrix and distention of the outer mitochondrial membrane (Sesso et al., 2012). This can lead to rupture of the outer mitochondrial membrane, thus releasing mitochondrial contents into the cytoplasm and initiating apoptosis.

The appearance of mitochondria in electron micrographs can vary depending on the section plane, which can lead to inaccurate measurements of mitochondrial sizes and shapes (Fig. 3). Stereology is a quantitative method that can be used to accurately measure the morphology of irregularly shaped objects, including mitochondria. This makes stereology a valuable tool for comparing mitochondria in different experimental and pathological conditions (Mandarim-de-Lacerda and Del Sol, 2017). Santuy et al. assessed the volume fraction encompassed by mitochondria, as well as their distribution among dendritic, axonal, and non-synaptic processes, through the application of Cavalieri's principle with stereological grids. Those authors employed a dual-beam electron microscope, which integrates a scanning electron microscope and a focused ion beam (Santuy et al., 2018). In another study, lipid droplet (lipid) content and skeletal muscle mitochondrial density calculations were performed on images captured using transmission electron microscopy (Broskey et al., 2013). The idea behind these studies involved calculating the ratio of the mitochondrial volume to the whole tissue volume (West, 2012).

Morphometric measurements, such as diameter, length, and shape, can be employed for assessing mitochondrial morphology with the use of the following stereological tools:

- Volume density: The volume density of mitochondria represents the fraction of the total cell volume that is occupied by mitochondria. This parameter can be used to assess the overall abundance of mitochondria in a cell.
- Numerical density per area: The numerical density of mitochondria per area represents the number of mitochondria per unit area of cell cytoplasm. This parameter can be used to assess the spatial distribution of mitochondria within a cell.

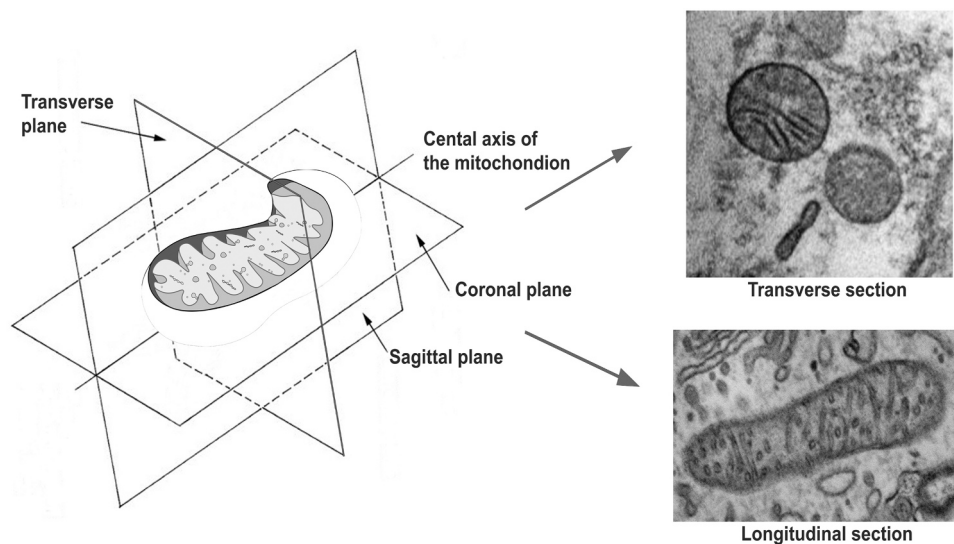


**Fig. 3.** : The appearance of the mitochondria in various orientations. Round-shaped mitochondria will be obtained from transverse plane sections, while coronal plane or sagittal plane sections will yield an elongated mitochondrion appearance.

- Cross-sectional area: The cross-sectional area of a mitochondrion represents the area of a slice through the mitochondrion at its widest point. This parameter can be used to assess the average size of mitochondria in a cell.
- Surface density: The surface density of a membrane represents the length of the membrane per unit area of cell cytoplasm. This parameter can be used to assess the surface area of mitochondrial membranes, such as the inner membrane, outer membrane, and cristae.

Measuring these parameters can yield valuable insights into the quantitative changes in mitochondrial morphology that occur under different experimental and pathological conditions (Fig. 4). For example, these parameters can be used to study how mitochondrial morphology changes in response to different metabolic stimuli, such as exercise or fasting, or to study how that morphology changes in different diseases, such as cancer or neurodegenerative diseases.

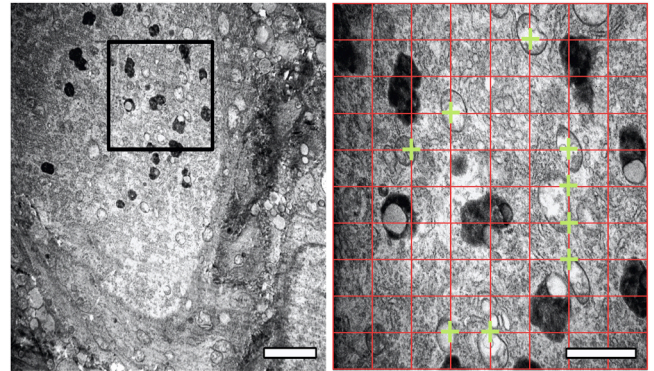


**Fig. 4.** Point counting test grid was performed at the electron microscopic level in order to estimate the reference volume ( $V_{ref}$ ). The proportion of points that intersect with mitochondria to the total number of points covering the entire area of the electron micrograph is indicated with green (+) signs. The total volume fraction of mitochondria can be estimated without requiring any knowledge of the area associated with each point on the grid or the magnification of the electron micrographs (bars: 2  $\mu\text{m}$ , 1  $\mu\text{m}$ , respectively).

### 1.6. Estimation of total sensory neuron numbers

Stereology and histomorphometry are two complementary methods for quantifying neuron characteristics in normal and diseased peripheral nerves. The use of the fractionator technique in combination with physical disector permits accurate evaluation of sensory neuron numbers in ganglion tissues. The disector counting technique (a volume probe) is advantageous over assumption-based methods as it involves directly counting objects within a specific structure volume, thereby eliminating potential biases. This method shares similarities with the counting methods used for serially reconstructed objects, as it does not rely on information about the objects' geometry. The conditions required for applying this technique are identical to those for making counts of serial reconstructions. The technique represents a practical and reliable approach that enables cell counts to be estimated independently of the structure's shape and size. In this method, analyses are conducted on sampled sections representing the tissue, and the results are multiplied by the sampling rates. The total cell count within the entire tissue can thus be estimated using a small portion/section representing the entire structure. Sections of disector pairs are obtained from the whole tissue based on a sampling interval determined through a pilot study (for the physical fractionator method, an average of 15–17 sampled sections pairs from each block will be sufficient). The disector technique is counted using an unbiased counting frame (Fig. 5). Particle number counting is performed within the virtual volume between the reference and look-up sections using an unbiased counting frame. The result is then multiplied by previously applied sampling fractions (section sampling, area sampling, and tissue sampling) to estimate the total cell number (Gundersen et al., 1988b).

The elimination of potential bias and improved efficiency have been significant considerations in the ongoing development of stereological methods (Gundersen and Jensen, 1987; Gundersen et al., 1999; Hosseini-Sharifabad and Nyengaard, 2007; West, 1999). The implementation of an unbiased sampling design in stereology, which involves the application of a set of uniformly random points, permits the estimation of reference volume ( $V_{ref}$ ) values while estimating density using the disector method. This approach offers the advantage that the total number ( $N$ ) estimation is not affected by any alterations in tissue volume, as all measurements are relative and expressed as fractions (Gundersen et al., 1988a; West, 1993, 2002). The disector method, using a random systematic sampling design, calculates the number of particles ( $N$ ) by counting the particles ( $Q^-$ ) within a known volume of tissue that represents a known fraction ( $f$ ) of the volume of the region of interest ( $V_{ref}$ ). The total number ( $N$ ) of particles within the reference volume ( $V_{ref}$ ) is determined by multiplying the number of particles counted ( $Q^-$ ) by the inverse of the fraction ( $f$ ), expressed as  $N = Q^- \times (1/f)$  (Fig. 5).

The disector, known as a 3D (volume) probe, consists of two consecutive sections with a known distance. The volume of the disector is determined by the distance between the corresponding surfaces of the two sections and the area sampled on one of the sections. When using disectors for counting, the objective is to determine whether a specific object is associated with a particular disector. In order to ensure equal probabilities for all objects, regardless of their size, shape, or orientation, rules are applied to associate objects with the volume defined by the disector. This is achieved by identifying a unique sampling point on or within an object and determining whether this falls within the disector probe. Reducing the object to a single sampling point eliminates considerations of its size, shape, and orientation. Various unique sampling points can be employed for counting objects in histological material, such as their leading edge. The leading edge refers to the point at which the object is first encountered when progressing through a series of sections. By applying this approach, each object will be counted only once.

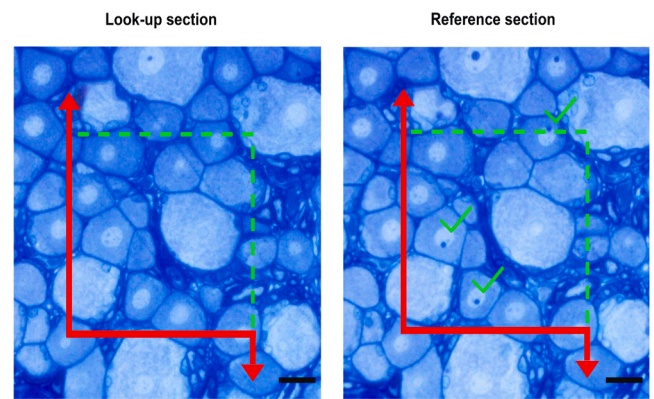


**Fig. 5.** Images showing the application of the physical disector technique in ganglion tissue. The researcher or software capture the matching fields and display them side-by-side. The cell is considered a countable object if it is present in the reference, but not in the look-up, section (red lines: exclusion lines; green lines: inclusion lines). In this application, we used nucleolus of ganglion cells as countable particle. Toluidine blue staining of the rat L5 ganglion tissue (bar: 20  $\mu$ m).

## 2. In conclusion

Stereological approaches are becoming a standard method for use in quantitative research. In addition to classic histological sections, the applicability of stereological methods in immunohistochemical sections, electron microscopic images, and confocal microscopic images is also growing. In parallel with future technology advancements, as stereological applications become simpler, quantitative assessments can be conducted more efficiently. The elucidation of cellular changes in dorsal root ganglia following peripheral nerve injury is crucial for understanding nerve degeneration and regeneration studies, as well as neuronal plasticity. The examination of dorsal root ganglion tissue is important for evaluating pathological processes in the sensory system and the morphological assessment of neuronal cell body responses exposed to mechanical stress.

Information obtained through reliable quantitative stereological techniques is crucial for the morphological or quantitative observation of cell degeneration. In addition to cell death following injury, the effectiveness of potential therapeutic agents can be rendered quantifiable with the use of stereological methods. Developing methods that enhance the survival of primary sensory neurons, and their description with numerical data, will become increasingly important in future studies.

### CRedit authorship contribution statement

**Vianney John-Mary:** Supervision, Writing – review & editing. **Kaplan Suleyman:** Writing – review & editing. **DELİBAŞ Burcu:** Writing – review & editing, Writing – original draft.

### Declaration of Competing Interest

There are no conflicts of interest for the authors.

### Data Availability

No data was used for the research described in the article.

### References

- Baddeley, A.J., Gundersen, H.J.G., Cruzorive, L.M., 1986. Estimation of surface-area from vertical sections. *J. Microsc.* 142, 259–276. <https://doi.org/10.1111/j.1365-2818.1986.tb04282.x>.



- Beiswanger, C.M., Roscoe-Graessle, T.L., Zerbe, N., Reuhl, K.R., Lowndes, H.E., 1993. 3-Acetylpyridine-induced degeneration in the dorsal root ganglia: involvement of small diameter neurons and influence of axotomy. *Neuropathol. Appl. Neurobiol.* 19, 164–172. <https://doi.org/10.1111/j.1365-2990.1993.tb00423.x>.
- Brantova, O., Tesarova, M., Hansikova, H., Elleder, M., Zeman, J., Sladkova, J., 2006. Ultrastructural changes of mitochondria in the cultivated skin fibroblasts of patients with point mutations in mitochondrial DNA. *Ultra Pathol.* 30, 239–245. <https://doi.org/10.1080/01913120600820112>.
- Broskey, N.T., Daraspe, J., Humbel, B.M., Amati, F., 2013. Skeletal muscle mitochondrial and lipid droplet content assessed with standardized grid sizes for stereology. *J. Appl. Physiol.* 115 (1985), 765–770. <https://doi.org/10.1152/jappphysiol.00063.2013>.
- Brown, D.L., Staup, M., Swanson, C., 2020. Stereology of the peripheral nervous system. *Toxicol. Pathol.* 48, 37–48. <https://doi.org/10.1177/0192623319854746>.
- Butt, M.T., 2010. Vacuoles in dorsal root ganglia neurons: some questions, 999–999. *Toxicol. Pathol.* 38. <https://doi.org/10.1177/0192623310378869>.
- Canan, S., Bozkurt, H.H., Acar, M., Vlamings, R., Aktas, A., Sahin, B., Temel, Y., Kaplan, S., 2008. An efficient stereological sampling approach for quantitative assessment of nerve regeneration. *Neuropathol. Appl. Neurobiol.* 34, 638–649. <https://doi.org/10.1111/j.1365-2990.2008.00938.x>.
- Carr, V.M., Simpson, S.B., Jr, 1978. Proliferative and degenerative events in the early development of chick dorsal root ganglia. II. Responses to altered peripheral fields. *J. Comp. Neurol.* 182, 741–755. <https://doi.org/10.1002/cne.901820411>.
- Cavaletti, G., Gilardini, A., Canta, A., Rigamonti, L., Rodriguez-Menendez, V., Ceresa, C., Marmiroli, P., Bossi, M., Oggioni, N., D'Incalci, M., De Coster, R., 2007. Bortezomib-induced peripheral neurotoxicity: a neurophysiological and pathological study in the rat. *Exp. Neurol.* 204, 317–325. <https://doi.org/10.1016/j.expneurol.2006.11.010>.
- Chadwick, W., Magnus, T., Martin, B., Keselman, A., Mattson, M.P., Maudsley, S., 2008. Targeting TNF-alpha receptors for neurotherapeutics. *Trends Neurosci.* 31, 504–511. <https://doi.org/10.1016/j.tins.2008.07.005>.
- Cragg, B.G., 1970. What is the signal for chromatolysis? *Brain Res.* 23, 1–21. [https://doi.org/10.1016/0006-8993\(70\)90345-8](https://doi.org/10.1016/0006-8993(70)90345-8).
- Delibas, B., Kaplan, S., 2023. The histomorphological and stereological assessment of rat dorsal root ganglion tissues after various types of sciatic nerve injury. *Histochem Cell Biol.* <https://doi.org/10.1007/s00418-023-02242-0>.
- Delibas, B., Kuruoglu, E., Bereket, M.C., Onger, M.E., 2021. Allantoin, a purine metabolite, enhances peripheral nerve regeneration following sciatic nerve injury in rats: a stereological and immunohistochemical study. *J. Chem. Neuroanat.* 117, 102002. <https://doi.org/10.1016/j.jchemneu.2021.102002>.
- Dentinger, M.P., Barron, K.D., Kohberger, R.C., McLean, B., 1979. Cytologic observations on axotomized feline Betz cells. II. Quantitative ultrastructural findings. *J. Neuropathol. Exp. Neurol.* 38, 551–564. <https://doi.org/10.1097/00005072-197909000-00008>.
- Engh, C.A., Schofield, B.H., 1972. A review of the central response to peripheral nerve injury and its significance in nerve regeneration. *J. Neurosurg.* 37, 195–203. <https://doi.org/10.3171/jns.1972.37.2.0195>.
- Felix, S.P., Pereira Lopes, F.R., Marques, S.A., Martinez, A.M., 2013. Comparison between suture and fibrin glue on repair by direct coaptation or tubulization of injured mouse sciatic nerve. *Microsurgery* 33, 468–477. <https://doi.org/10.1002/micr.22109>.
- Feng, R., Muraleedharan Saraswathy, V., Mokalled, M.H., Cavalli, V., 2023. Self-renewing macrophages in dorsal root ganglia contribute to promote nerve regeneration. *Proc. Natl. Acad. Sci. USA* 120, e2215906120. <https://doi.org/10.1073/pnas.2215906120>.
- Gehrmann, J., Monaco, S., Kreutzberg, G.W., 1991. Spinal cord microglial cells and DRG satellite cells rapidly respond to transection of the rat sciatic nerve. *Restor. Neurol. Neurosci.* 2, 181–198. <https://doi.org/10.3233/RNN-1991-245605>.
- Geuna, S., 2015. The sciatic nerve injury model in pre-clinical research. *J. Neurosci. Methods* 243, 39–46. <https://doi.org/10.1016/j.jneumeth.2015.01.021>.
- Gorman, G.S., Chinnery, P.F., DiMauro, S., Hirano, M., Koga, Y., McFarland, R., Suomalainen, A., Thorburn, D.R., Zeviani, M., Turnbull, D.M., 2016. Mitochondrial diseases. *Nat. Rev. Dis. Prim.* 2, 16080. <https://doi.org/10.1038/nrdp.2016.80>.
- Grothe, C., Meisinger, C., Hertenstein, A., Kurtz, H., Wewetzer, K., 1997. Expression of fibroblast growth factor-2 and fibroblast growth factor receptor 1 messenger RNAs in spinal ganglia and sciatic nerve: regulation after peripheral nerve lesion. *Neuroscience* 76, 123–135. [https://doi.org/10.1016/s0306-4522\(96\)00355-7](https://doi.org/10.1016/s0306-4522(96)00355-7).
- Guimaraes, R.M., Anibal-Silva, C.E., Davoli-Ferreira, M., Gomes, F.I.F., Mendes, A., Cavallini, M.C.M., Fonseca, M.M., Damasceno, S., Andrade, L.P., Colonna, M., Rivat, C., Cunha, F.Q., Alves-Filho, J.C., Cunha, T.M., 2023. Neuron-associated macrophage proliferation in the sensory ganglia is associated with peripheral nerve injury-induced neuropathic pain involving CX3CR1 signaling. *Elife* 12. <https://doi.org/10.7554/eLife.78515>.
- Gundersen, H.J.G., Bagger, P., Bendtsen, T.F., Evans, S.M., Korbo, L., Marcussen, N., Moller, A., Nielsen, K., Nyengaard, J.R., Pakkenberg, B., Sorensen, F.B., Vesterby, A., West, M.J., 1988a. The new stereological tools - disector, fractionator, nucleator and point sampled intercepts and their use in pathological research and diagnosis. *Apmis* 96, 857–881. <https://doi.org/10.1111/j.1699-0463.1988.tb00954.x>.
- Gundersen, H.J.G., Bendtsen, T.F., Korbo, L., Marcussen, N., Moller, A., Nielsen, K., Nyengaard, J.R., Pakkenberg, B., Sorensen, F.B., Vesterby, A., West, M.J., 1988b. Some new, simple and efficient stereological methods and their use in pathological research and diagnosis - review article. *Apmis* 96, 379–394. <https://doi.org/10.1111/j.1699-0463.1988.tb05320.x>.
- Gundersen, H.J.G., Jensen, E.B., 1987. The efficiency of systematic-sampling in stereology and its prediction. *J. Microsc.-Oxf.* 147, 229–263. <https://doi.org/10.1111/j.1365-2818.1987.tb02837.x>.
- Gundersen, H.J.G., Jensen, E.B.V., Ki u, K., Nielsen, J., 1999. The efficiency of systematic sampling in stereology-reconsidered. *J. Microsc.* 193, 199–211. <https://doi.org/10.1046/j.1365-2818.1999.00457.x>.
- Hall, A.K., Landis, S.C., 1992. Division and migration of satellite glia in the embryonic rat superior Cervical-Ganglion. *J. Neurocytol.* 21, 635–647. <https://doi.org/10.1007/Bf01191725>.
- Hosseini-Sharifabad, M., Nyengaard, J.R., 2007. Design-based estimation of neuronal number and individual neuronal volume in the rat hippocampus. *J. Neurosci. Methods* 162, 206–214. <https://doi.org/10.1016/j.jneumeth.2007.01.009>.
- Humbertson, A., Jr., Zimmermann, E., Leedy, M., 1969. A chronological study of mitotic activity in satellite cell hyperplasia associated with chromatolytic neurons. *Z. Zellforsch. Mikros Anat.* 100, 507–515. <https://doi.org/10.1007/Bf00344371>.
- Iwai, H., Ataka, K., Suzuki, H., Dhar, A., Kuramoto, E., Yamanaka, A., Goto, T., 2021. Tissue-resident M2 macrophages directly contact primary sensory neurons in the sensory ganglia after nerve injury. *J. Neuroinflamm.* 18, 227. <https://doi.org/10.1186/s12974-021-02283-z>.
- Jensen, E.B.V., Gundersen, H.J.G., 1993. The rotator. *J. Microsc.-Oxf.* 170, 35–44. <https://doi.org/10.1111/j.1365-2818.1993.tb03321.x>.
- Lawrence, T., 2009. The nuclear factor NF-kappaB pathway in inflammation. *Cold Spring Harb. Perspect. Biol.* 1, a001651. <https://doi.org/10.1101/cshperspect.a001651>.
- Levy Bde, F., Cunha Jdo, C., Chadi, G., 2007. Cellular analysis of S100Beta and fibroblast growth factor-2 in the dorsal root ganglia and sciatic nerve of rodents. focus on paracrine actions of activated satellite cells after axotomy. *Int. J. Neurosci.* 117, 1481–1503. <https://doi.org/10.1080/15569520701502716>.
- Li, S., Xue, C., Yuan, Y., Zhang, R., Wang, Y., Wang, Y., Yu, B., Liu, J., Ding, F., Yang, Y., Gu, X., 2015. The transcriptional landscape of dorsal root ganglia after sciatic nerve transection. *Sci. Rep.* 5, 16888. <https://doi.org/10.1038/srep16888>.
- Lieberman, A.R., 1971. The axon reaction: a review of the principal features of perikaryal responses to axon injury. *Int. Rev. Neurobiol.* 14, 49–124. [https://doi.org/10.1016/s0074-7742\(08\)60183-x](https://doi.org/10.1016/s0074-7742(08)60183-x).
- Mandarin-de-Lacerda, C.A., Del Sol, M., 2017. Tips for studies with quantitative morphology (Morphometry and Stereology). *Int. J. Morphol.* 35, 1482–1494. <https://doi.org/10.4067/S0717-95022017000401482>.
- Melli, G., Taiana, M., Camozzi, F., Triolo, D., Podini, P., Quattrini, A., Taroni, F., Lauria, G., 2008. Alpha-lipoic acid prevents mitochondrial damage and neurotoxicity in experimental chemotherapy neuropathy. *Exp. Neurol.* 214, 276–284. <https://doi.org/10.1016/j.expneurol.2008.08.013>.
- Pannese, E., 1960. Observations on the morphology, submicroscopic structure and biological properties of satellite cells (s.c.) in sensory ganglia of mammals. *Z. Zellforsch. Mikros Anat.* 52, 567–597. <https://doi.org/10.1007/Bf00339847>.
- Pannese, E., 1981. The satellite cells of the sensory ganglia. *Adv. Anat. Embryol. Cell Biol.* 65, 1–111. <https://doi.org/10.1007/978-3-642-67750-2>.
- Sandelin, M., Zabih, S., Liu, L., Wicher, G., Kozlova, E.N., 2004. Metastasis-associated S100A4 (Mts1) protein is expressed in subpopulations of sensory and autonomic neurons and in Schwann cells of the adult rat. *J. Comp. Neurol.* 473, 233–243. <https://doi.org/10.1002/cne.20115>.
- Santuy, A., Turegano-Lopez, M., Rodriguez, J.R., Alonso-Nanclares, L., DeFelipe, J., Merchan-Perez, A., 2018. A quantitative study on the distribution of mitochondria in the neuropil of the juvenile rat somatosensory cortex. *Cereb. Cortex* 28, 3673–3684. <https://doi.org/10.1093/cercor/bhy159>.
- Seddon, H.J., 1942. A classification of nerve injuries. *Br. Med. J.* 2, 237–239. <https://doi.org/10.1136/bmj.2.4260.237>.
- Serger, E., Luengo-Gutierrez, L., Chadwick, J.S., Kong, C., Zhou, L., Crawford, G., Danzi, M.C., Myridakis, A., Brandis, A., Bello, A.T., Muller, F., Sanchez-Vassopoulos, A., De Virgiliis, F., Liddell, P., Dumas, M.E., Strid, J., Mani, S., Dodd, D., Di Giovanni, S., 2022. The gut metabolite indole-3 propionate promotes nerve regeneration and repair. *Nature* 607, 585–592. <https://doi.org/10.1038/s41586-022-04884-x>.
- Sesso, A., Belizario, J.E., Marques, M.M., Higuchi, M.L., Schumacher, R.I., Colquhoun, A., Ito, E., Kawakami, J., 2012. Mitochondrial swelling and incipient outer membrane rupture in preapoptotic and apoptotic cells. *Anat. Rec.* 295, 1647–1659. <https://doi.org/10.1002/ar.a.22553>.
- Sonmez, O.F., Odaci, E., Bas, O., Colakoglu, S., Sahin, B., Bilgic, S., Kaplan, S., 2010. A stereological study of MRI and the Cavalieri principle combined for diagnosis and monitoring of brain tumor volume. *J. Clin. Neurosci.* 17, 1499–1502. <https://doi.org/10.1016/j.jocn.2010.03.044>.
- Su, W.F., Wu, F., Jin, Z.H., Gu, Y., Chen, Y.T., Fei, Y., Chen, H., Wang, Y.X., Xing, L.Y., Zhao, Y.Y., Yuan, Y., Tang, X., Chen, G., 2019. Overexpression of P2X4 receptor in Schwann cells promotes motor and sensory functional recovery and remyelination via BDNF secretion after nerve injury. *Glia* 67, 78–90. <https://doi.org/10.1002/glia.23527>.
- Sunderland, S., 1951. A classification of peripheral nerve injuries producing loss of function. *Brain* 74, 491–516. <https://doi.org/10.1093/brain/74.4.491>.
- Takeda, M., Tanimoto, T., Kadoi, J., Nasu, M., Takahashi, M., Kitagawa, J., Matsumoto, S., 2007. Enhanced excitability of nociceptive trigeminal ganglion neurons by satellite glial cytokine following peripheral inflammation. *Pain* 129, 155–166. <https://doi.org/10.1016/j.pain.2006.10.007>.
- Terry, R.D., DeTeresa, R., Hansen, L.A., 1987. Neocortical cell counts in normal human adult aging. *Ann. Neurol.* 21, 530–539. <https://doi.org/10.1002/ana.410210603>.
- Wallace, D.C., 1999. Mitochondrial diseases in man and mouse. *Science* 283, 1482–1488. <https://doi.org/10.1126/science.283.5407.1482>.
- Wee Yong, V., 2010. Inflammation in neurological disorders: a help or a hindrance? *Neuroscientist* 16, 408–420. <https://doi.org/10.1177/1073858410371379>.
- West, M.J., 1993. New stereological methods for counting neurons. *Neurobiol. Aging* 14, 275–285. [https://doi.org/10.1016/0197-4580\(93\)90112-0](https://doi.org/10.1016/0197-4580(93)90112-0).

- West, M.J., 1999. Stereological methods for estimating the total number of neurons and synapses: issues of precision and bias. *Trends Neurosci.* 22, 51–61. [https://doi.org/10.1016/s0166-2236\(98\)01362-9](https://doi.org/10.1016/s0166-2236(98)01362-9).
- West, M.J., 2002. Design-based stereological methods for counting neurons. *Prog. Brain Res.* 135, 43–51.
- West, M.J., 2012. Estimating volume in biological structures. *Cold Spring Harb. Protoc.* 2012, 1129–1139. <https://doi.org/10.1101/pdb.top071787>.
- Xian, C.J., Zhou, X.F., 1999. Neuronal-gliial differential expression of TGF- $\alpha$  and its receptor in the dorsal root ganglia in response to sciatic nerve lesion. *Exp. Neurol.* 157, 317–326. <https://doi.org/10.1006/exnr.1999.7063>.
- Yu, X.B., Liu, H.J., Hamel, K.A., Morvan, M.G., Yu, S., Leff, J., Guan, Z.H., Braz, J.M., Basbaum, A.I., 2020. Dorsal root ganglion macrophages contribute to both the initiation and persistence of neuropathic pain. *Nat. Commun.* 11. ARTN 264. [10.1038/s41467-019-13839-2](https://doi.org/10.1038/s41467-019-13839-2).
- Zhang, J.M., Donnelly, D.F., Song, X.J., Lamotte, R.H., 1997. Axotomy increases the excitability of dorsal root ganglion cells with unmyelinated axons. *J. Neurophysiol.* 78, 2790–2794. <https://doi.org/10.1152/jn.1997.78.5.2790>.
- Zhang, Y., Roslan, R., Lang, D., Schachner, M., Lieberman, A.R., Anderson, P.N., 2000. Expression of CHL1 and L1 by neurons and glia following sciatic nerve and dorsal root injury. *Mol. Cell Neurosci.* 16, 71–86. <https://doi.org/10.1006/mcne.2000.0852>.